



Investigating net primary production in climate regions of Khuzestan Province, Iran using CASA model

Afsaneh Afzali¹ · Fatemeh Hadian² · Soheil Sabri³ · Leila Yaghmaei²

Received: 10 May 2023 / Revised: 20 March 2024 / Accepted: 1 April 2024 / Published online: 16 May 2024
© The Author(s) under exclusive licence to International Society of Biometeorology 2024

Abstract

This study aimed to investigate the vegetation production changes in Khuzestan province, Iran using MODIS data production, meteorological data, vegetation maps as well as topographic and field monitoring data in CASA model. The study area was divided into different climatic classes based on multivariate statistical method, so the vegetation of each climatic region was examined separately for changes in NPP values. Production changes due to degradation were calculated using the Miami model and subsequently, the rain use efficiency (RUE) and the light use efficiency (LUE) and correlation indices between the CASA model and ground data were determined. The results of this study (R^2) showed that the accuracy of this model varies depending on the type of climatic regions ($R^2=0.80$ to $R^2=0.15$). In different climatic regions, the rate of NPP changes (very humid 68 gC/m^2 to ultra-dry 15 gC/m^2) varies in rangeland types. The highest rate of vegetation production is observed seasonally in May. Degradation conditions also reduced RUE and LUE. However, in hyper-arid regions, adaptations of plants in some different species (*Hammada Spp.*) increase their efficiency compared to other vegetation types. The results showed the importance of vegetation and climate classification in vegetation production studies.

Keywords Climate type · NPP · Satellite imagery · CASA model

Introduction

The United Nations (UN), through the sustainable development goal 13 (SDG13), urged member nations to take urgent action to combat climate change and its impacts. One of the major impacts of climate change is decreasing vegetation and food production, which has implications for food security (UN, 2015). This issue is more apparent in arid and semi-arid lands, where there is a high vulnerability to unpredictable weather change patterns and scarce resources. Many countries worldwide adopted mitigation measures through monitoring the Net Primary Production (NPP) estimation of plants in different climatic regions. This process facilitates

fostering the process of decision making and policy making in resource allocation and foreseeing the potential treats to address before impacting the societies. As an example, NPP estimation and its comparison in different climatic regions have been used to inform the impact of climate change on vegetation production and, accordingly, an indicator for decision-making on future food security measures (UN, 2020).

The NPP indicates the difference between photosynthesis or gross production and plant respiration, which can explain the state of the carbon cycle and how carbon dioxide is stabilized (Ruimy et al. 1999). The NPP value is one of the most essential quantitative characteristics of the biosphere. Production rates of vegetation in any ecosystem are affected by climatic factors such as temperature (Han et al. 2023a, b), precipitation, soil conditions, solar energy, and living organisms, which vary significantly on a seasonal and annual scale (Imhoff et al. 2004). Therefore, the amount of NPP is essential in terms of the amount of matter for the second levels of the food chain and a sign of ecosystem health, ecological balance, and a carbon fixation source (Costanza 2012).

Therefore, studying the relationship between climate change and the amount of NPP is one of the basic principles

✉ Afsaneh Afzali
a.afzali@kashanu.ac.ir

¹ Department of Environment, Faculty of Natural Resources and Earth Sciences, University of Kashan, Kashan, Iran

² Department of Natural Resources, Isfahan University of Technology, Isfahan, Iran

³ Center for Spatial Data Infrastructures and Land Administration, The University of Melbourne, Melbourne, Australia

of environmental studies (Wang et al. 2022; Han et al. 2023a, b). In research studies of climate impact on NPP at various global or regional levels, the interaction between ecosystems and climate change has been studied (Cramer et al. 2001). The amount of NPP is also referred to as the rate of carbohydrate stabilization in plant tissues and is defined as the rate of gross primary production regardless of plant respiration. Changes in NPP values have been investigated from various aspects such as climate and spatial and temporal distribution (Chen et al. 1999) on different geographical scales. Although the amount of vegetation production and carbon stabilization can be measured through land surveys, there are many limitations in traditional methods for various reasons, such as their cost-effectiveness and time-consuming nature and the generalization of results in the large area.

Over the last two decades, technological advancements such as remote sensing and modeling addressed the cost-effectiveness and tedious workflow challenges of land surveying in extended areas. Using such technological developments alongside field works allowed collecting more reliable ecological data and results (Khajeddin 1995; Darvish Sefat and Zare 1998; Bajgirani et al. 2008). In recent years, various models have been proposed to estimate the NPP, including models based on the carbon cycle and plant structure (He et al. 2018). These remote sensing models can be categorized into three groups of 1) statistical, 2) parametric, and 3) process-based, which make it possible to study spatial and temporal changes in NPP (Ruimy et al. 1994). For instance, the CASA is a process-based model that considers the efficiency of solar energy absorption with the help of remote sensing and climate measurement data. This model estimates the NPP value on a regional and global scale. The CASA model uses monthly climatic data of temperature, precipitation, and sunshine hours of NDVI3 data and land cover maps (Zhang et al. 2017). The CASA model as a process-oriented model has a remarkable ability to reveal temporal and spatial patterns combining climatic and terrestrial information simulates changes in the NPP situation (Deyong et al., 2009).

However, due to the need for soil moisture parameter and the limitations of its determination on various scales in the CASA model, further methods should be applied to ensure the reliability of results. For instance, in the case of the error measurement between observed and modeled NPP, light use efficiency (LUE) value can be calculated, and exchanging carbon dioxide between the atmosphere and carbon sequestration can be modeled (Bradford et al. 2005; Yu et al. 2009). The LUE is an influential factor in converting absorbable energy into organic matter and is a critical factor in measuring NPP with the CASA model. Evaluation of the CASA model at the global (Field et al. 1995) and regional (Peng et al. 2016) levels has shown that

it is possible to estimate NPP values according to climatic conditions and plant type.

The effects of land degradation can also be examined at different stages of phenology (Dieguez & Paruelo 2017). According to observations (Fischer et al. 2014), the LUE value of plants was maximum in the optimal environmental conditions. Still, factors such as temperature, humidity, pests and diseases, soil nutrients, and genetic and morphological characteristics of plants (i.e., leaf area index) greatly impacted it. Therefore, it is not the same amount in different plant types. Yaghmaei et al. (2021) studied the estimation of NPP in the climatic regions of the Central Zagros of Iran using the CASA model and meteorological data. NPP, LUE, and (rain use efficiency) RUE were extracted from MODIS images and climatic data using CASA and Miami models. The spatial distribution of NPP and RUE showed that NPP and photosynthetic efficiency in degraded rangelands with poor and very poor conditions presented a greater decrease than the rangelands with a better condition. Some studies have also investigated the extent of NPP changes in a part of the African continent (Fu et al. 2023), China (He et al. 2023; Chen et al. 2023), Mongolia (Ke et al. 2022), and Tibetan Plateau (Zha et al. 2022).

Due to the vastness of the rangelands, their impassability, and the speed of vegetation changes, the use of field methods alone cannot be used, and the modeling of vegetation in different climates and conditions of rangelands also needs to be investigated. On the other hand, the use of global models of net primary production in arid and semi-arid regions of Iran has some limitations (Yuan et al. 2006), and vegetation modeling with the help of MODIS images in some arid regions is not appropriately accurate (Gao et al. 2015). Iran is located in the Middle East between Caspian Sea and Oman Sea. The Alborz (in the north) and Zagros (in the west) ranges have created diverse climates in the country, so that the highest average annual rainfall is observed in Anzali port (2000 mm) and the lowest in Yazd (60 mm).

The changes in climatic regions play an important role in vegetation production (Han et al. 2023a, b), but due to the lack of sufficient land information in different climates of Iran, the modeling of NPP using the CASA model in various geographical conditions has not been done. Climate classification in studies can also play a significant role in the possibility of examining the level of NPP. Therefore, studying an area with high climatic diversity and accurate field data can illustrate the potential of modeling NPP.

Khuzestan province has different height altitudes and diverse climates from very humid and cold to ultra-dry, which is due to being located next to the Zagros ranges and plains. The study area is also located in a coastal area which related studies have been rarely performed in similar areas.

This climate condition has led to the emergence of various plant species with different vegetative forms that have good to very poor rangeland status. Therefore, the main purpose of this study is to investigate and model the NPP in plant types in the rangelands of Khuzestan province with the help of MODIS images and to evaluate the efficiency of plant photosynthesis in different climates of this region. The present study was conducted specifically to map NPP of Khuzestan province with the CASA model over a 21-year period from 2000–2021 along with its accuracy evaluation adopting field data on the scale of the climate zones.

Materials and methods

Study area

The study area located in the latitude 47° 41′ to 50° 39′ and latitude 29° 58′ to 33° 04′ and covers an area of about 64,236 square kilometers in Khuzestan province, Iran. This region includes different climatic regions in south-western Iran (Fig. 1). The region's average annual rainfall is 285 mm, where the air dryness increases from the north to the south by reducing the altitude. The highest and lowest recorded rainfall observed in Izeh and Abadan meteorological stations are 614 mm and 150 mm, respectively. The northern parts have a humid climate, but the southern parts have a hot and dry climate. The average annual temperature in this region is 27.6 °C, the absolute maximum is 53.7 °C, and the absolute minimum is -8.4 °C. In this area, about 500 hectares of vegetation are forests and 2.5 million hectares are rangelands. About 95% of the forests are Oak and the rest are other trees. In the rangelands of the province, 10% is good, 30% is poor and the rest have been degraded.

Meteorological data

In the present study, the adopted meteorological stations' data relating to rain gauges, climatology, and synoptic were extracted for studied province and neighboring regions. The data used in the CASA model include monthly temperature, precipitation, and hours of sunshine. The amount of solar energy was calculated using the sum of the hours of sunshine recorded at synoptic meteorological stations and the Angstrom- Prescott relationship (Alamdari et al., 2013). To prepare climatic maps, digital elevation models (DEM) and the relationship between climatic factors and topography were used.

Vegetation field data

The study intended to evaluate the amount of vegetation production. So, after homogenizing the areas from the soil and vegetation points of view, all rangeland vegetation productions in plant types with different rangeland conditions was measured in 4-pixel method in 2021 (Khaleghi and Aeinebeygi, 2016). In each plant type, 35 sites were determined, and at an area of 500 × 500 m² with 8 plots of 10 × 10 m², the percentage of perennial shrub was measured, and the annual production amount of all plant species was cut and weighed in 1 × 2 m² plots (Yeganeh et al., 2014). In perennial plants, only the current year's growth and in the case of wheat and annual plants, the entire harvested biomass on the ground was cut off. The sampling level was determined by considering the resolution of the MODIS satellite with 250*250 m², according to Eq. 1, where A is the sampling level, P is the pixel resolution of the satellite in meter, and L is the acceptable error (McCoy, 2005).

$$A = P \times (1 + 2L) \quad (1)$$

The condition of rangelands in Khuzestan province was adjusted using the 4-factor method, and the relevant forms were evaluated (Khaleghi & Aeinebeygi, 2016). In the 4-factor method, the factors of soil (with a score of 0–20), percentage of vegetation (with a score of 0–10), plant composition (with a score of 0–10), and vigor and freshness (with a score of 0–10) were evaluated. The sum of the scores reflecting the status of the rangeland was categorized. At a score above 45 degrees, the condition of the rangeland was excellent, 45–38 was good, 37–31 was moderate, 30–21 was poor, and less than 20 was very poor (Friedel, 1991). In Khuzestan province, the situation of rangelands was measured to be good to very poor.

Satellite data

In the present study, to determine NPP, the MODIS satellite, Terra sensor, were used, which could be downloaded from <https://earthexplorer.usgs.gov> (Behnke & Doescher, 2015). The amount of NPP in two spatial scales were provided with MODIS images with a resolution of 250*250 m². MODIS data included MOD13Q1 products available on a 16-day scale (2000–2021). Using remote sensing, the relevant processing and calibration were performed (Pack, 2009), which included geometric correction on MOD13Q1 products (Antunes et al., 2011). Measurement of NDVI was performed on a monthly basis by averaging 16-day images (Li et al., 2015). The NDVI index was calculated using Eq. 2.

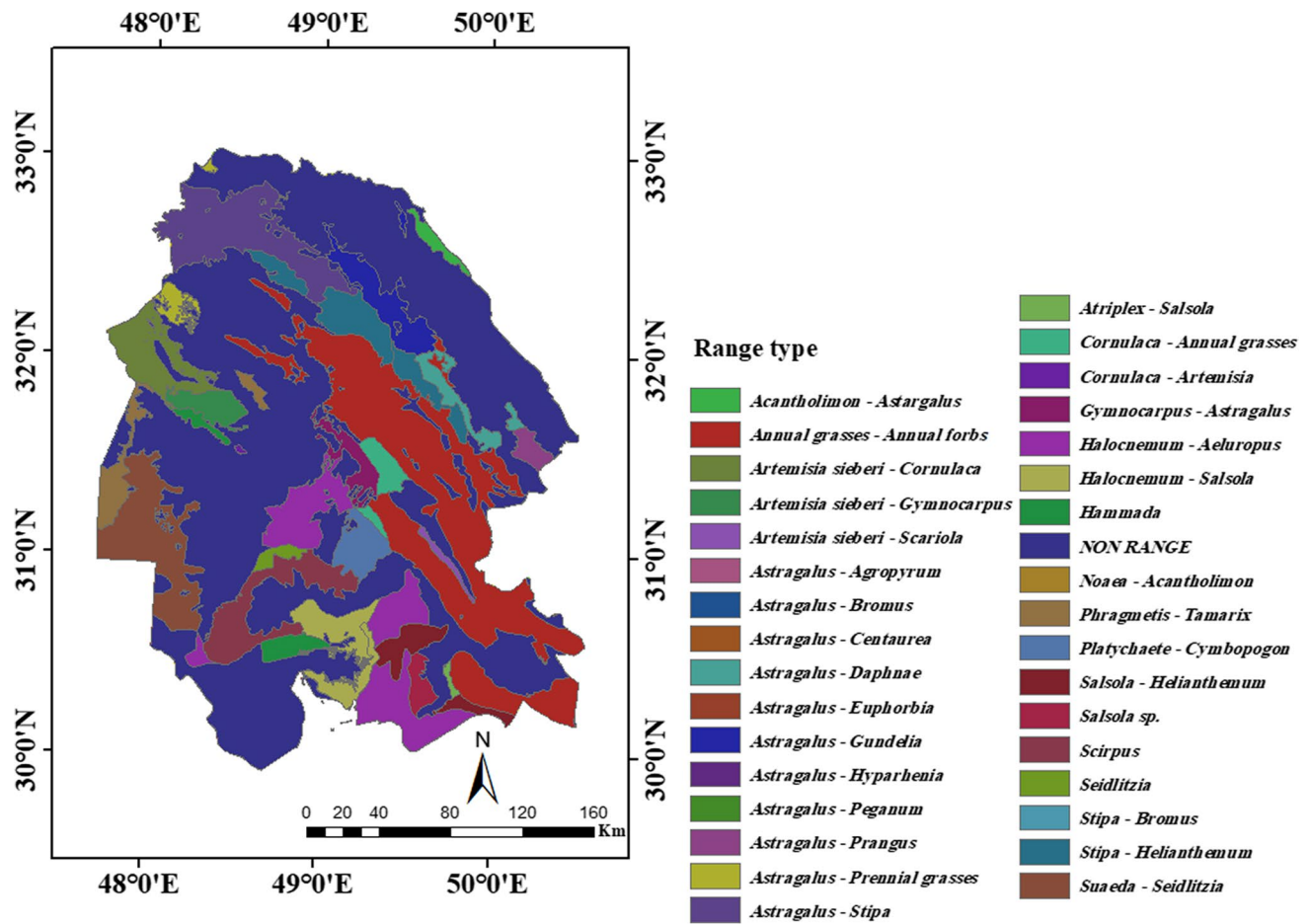


Fig. 1 Location of the study area in the country and on rangeland type map

$$NDVI = \frac{\rho_{NIR} - \rho_{red}}{\rho_{NIR} + \rho_{red}} \quad (2)$$

In Eq. 2, ρ_{NIR} is the amount of reflection in the near-infrared band with a wavelength of 867–841 nm in the band 2 of MODIS and ρ_{red} is as a reflection value in the red band with a wavelength of 670–620 nm in the band 1 of MODIS (Carlson & Ripley, 1997).

The prediction of NPP using CASA model

To implement the CASA model, meteorological parameters including precipitation, temperature, number of sunshine hours, NDVI index, and active photosynthetic adsorption ratio in 0.4–0.7 nm wavelength were considered. In doing so, land use and vegetation map (250,000 scale), which were validated by field observation, were used. The pixel size of all climate maps was determined to be 250*250 m² in line with the images of NDVI Index (Hua et al., 2014). The NPP for different vegetation types was determined separately. The relationship between the measured and estimated NPP in the

study sites was calculated using linear regression analysis, and the value of the coefficient of explanation and its statistical significance were determined. The Eqs. 3 and 4 are used in the CASA model where NPP, Absorbed Photosynthetically Active Radiation (APAR), and ϵ are net primary production, absorbed photosynthetically active radiation and light use efficiency.

$$NPP(x, t) = APAR(x, t) \times \epsilon(x, t) \quad (3)$$

$$APAR(x, t) = SOL(x, t) \times FPAR(x, t) \times 0.5 \quad (4)$$

Equations 5–12 show the calculation of Fraction of Absorbed Photosynthetically Active Radiation (FPAR) and the LUE. In Eqs. 5, 6, and 8, FPAR and SOL show the fraction of absorbed photosynthetically active radiation and the amount of sunlight, respectively. In Eqs. 6 and 8, the values of FPAR min and FPAR max are 0.001 and 0.95, respectively, and the FPAR value was calculated according to the relationship 5 and α where α was determined as the value of 0.475 based on the average of FPAR1 and FPAR2 (Yu et al. 2009).

$$FPAR(x, t) = \alpha \times FPAR_{NDVI} + (1 - \alpha) \times FPAR_{SR} \tag{5}$$

$$\alpha(x) = (0.651 \times I(x)^3 - 77.1 \times I(x)^2 + 17920 \times I(x) + 492390) \times 10^{-6} \tag{16}$$

$$FPAR(x, t) = \frac{(NDVI(x, t) - NDVI_{min}) \times (FPAR_{max} - FPAR_{min})}{(NDVI_{max} - NDVI_{min})} + FPAR_{min} \tag{6}$$

$$I(X) = \sum_{i=1}^{12} \left(\frac{T_{ai}}{5} \right)^{1.514} \tag{17}$$

$$SR = \left(\frac{1 + NDVI(x, t)}{1 - NDVI(x, t)} \right) \tag{7}$$

$$FPAR(x, t) = \frac{(SR(x, t) - SR_{min}) \times (FPAR_{max} - FPAR_{min})}{(SR_{max} - SR_{min})} + FPAR_{min} \tag{8}$$

$$\epsilon(x, t) = T_{\epsilon 1}(x, t) \times T_{\epsilon 2}(x, t) \times W_{\epsilon}(x, t) \times \epsilon_{max} \tag{9}$$

$$T_{\epsilon 1}(x, t) = 0.8 + 0.02T_{opt}(x) - 0.0005 \times [T_{opt}(x)]^2 \tag{10}$$

$$T_{\epsilon 2}(x, t) = 1.184 / \{1 + \exp[0.2 \times (T_{opt}(x) - 10 - T(x, t))]\} \times 1 / \{1 + \exp[0.3 \times (-T_{opt}(x) - 10 - T(x, t))]\} \tag{11}$$

$$W_{\epsilon}(x, t) = 0.5 + 0.5 \times \left[\frac{E(x, t)}{P(x, t)} \right] \tag{12}$$

In Eqs. 3 and 9 ϵ_{max} indicates the maximum light utilization efficiency and ϵ is the light utilization efficiency. The top t value is the average monthly temperature at a time of year when the NDVI index has the highest value. $T_{\epsilon 1}$ is the temperature at which the plant can perform its photosynthetic activity, $T_{\epsilon 2}$ is the temperature at which the plant can make effective use of sunlight, and W_{ϵ} is water stress coefficient in the effective use of radiation. The amount of W_{ϵ} is determined by the moisture holding capacity of the soil, which was calculated based on the actual evaporation ratio on the potential evaporation. In the Eqs. 13, 14, and 15, E is the rate of evaporation in the region, Ep is the regional potential evapotranspiration, Eo is the local potential evapotranspiration, R is the effective radiation of the sun and I is the annual heat index (Rohli & Vega, 2013). Therefore, the monthly NPP was calculated using Eqs. 3–17 and the annual values were obtained by summing the monthly values.

$$E(x, t) = \frac{\{P \times R(x, t) \times [P^2 + (R(x, t))^2 + P \times R(x, t)]\}}{\{[P + R(x, t)] \times [P^2 + R(x, t)]\}} \tag{13}$$

$$P(x, t) = [E(x, t) + E_0(x, t)] / 2 \tag{14}$$

$$E_0(x, t) = 16 \times \left[\frac{10 \times T(x, t)}{I(x)} \right]^{\alpha(x)} \tag{15}$$

Calculating the LUE

Determining the amount of effective solar radiation based on the thermodynamics law and the ratio of the output energy (NPP value) to the input (solar energy) is performed as the efficiency of light consumption (Eq. 18). The LUE value is considered as the line slope in the regression relationship between APAR (value x) and observational NPP (value y).

$$LUE = \frac{NPP}{APAR} \tag{18}$$

Effects of climatic and human factors on NPP

Vegetation type and cover in each region is the result of the interaction of climate and human activities. In the present study, the CASA model was used to measure the actual NPP using climatic and vegetative parameters. The Miami model was used to calculate potential NPP, which with the help of the least sum of regression squares, the amount of changes of potential NPP was calculated (Zhou et al. 2014).

The potential of NPP

The Miami model was used to determine the potential of NPP in the region. This model was first presented by Lieth at the Miami Conference (1972). In this model, with the help of meteorological data such as precipitation and temperature, the potential of NPP was determined in order to eliminate the effect of humans and other organisms on NPP. This model can be used for different climate conditions (Lieth 1975). Equation 19 shows potential NPP.

$$NPP = 3000 \times [1 - e^{0.0009695(v-20)}] \tag{19}$$

$$V = \frac{1.05 \times r}{\sqrt{1 + (1 + 1.05 \times r/L)}}$$

$$L = 3000 \times 25t + 0.05t^3$$

where NPP is the amount of the potential of NPP, V is the average annual actual evapotranspiration, L is the average annual potential evapotranspiration, r is the total annual precipitation and t is the average annual temperature.

The investigation of RUE index

In order to determine the effects of rainfall and rangeland degradation on vegetation production, the RUE index was calculated based on the ratio between NPP values to the amount of rainfall received. For this purpose, the average NPP (annual) map was divided by the average annual rainfall (2000–2016) over a period of 17 years. It was extracted for different vegetation types (Zhang et al. 2014). Equation 20 shows rain use efficiency.

$$RUE = \frac{NPP}{Rain} \quad (20)$$

Results

Evaluation of the CASA model in the study of NPP

Examination of the correlation between ground data and CASA model showed that there is a relatively good relationship in the study area between observed and simulated

data (Tables 1, 2, 3 and 4). According to the results, the correlation between the measured data and the CASA model varies depending on the type of climate conditions. The highest correlation was observed in very humid climate and the lowest correlation was observed in ultra-dry climate. According to the observations, the correlation between CASA model and NPP was 0.81 to 0.15 in very humid to hyper-arid regions. In very humid regions, the highest correlation between vegetation production and CASA model was in *Amygdalus scoparia* (0.81), while there was a decrease in rangeland types compared to forest areas.

In the humid climate region, the correlation between terrestrial data and the CASA model was reduced compared to the very humid climate. The highest correlation was found in *Amygdalus scoparia* (0.79) and the lowest was observed in *Astragalus Spp.–Prennial grasses*(0.61). The correlation between plant types and CASA model decreased with climate drying. Thus, in semi-humid climates, *Amygdalus scoparia* (0.75) was calculated as the highest and *Astragalus Spp.–Prennial grasses* (0.43) as the lowest in Mediterranean climates, *Quercus brantii* (0.74) was calculated as the highest and *Stipa Spp. – Helianthemum Spp.* (0.38) as the

Table 1 The values of NPP, RUE, LUE, correlation between terrestrial data and CASA model (R^2) and percentage of NPP potential used in plant types of humid climate

NO	Vegetation type	Life form (range condition)	NPP (gC/m ²)	LUE	RUE	R ²	NPP Change
1	<i>Amygdalus scoparia</i>	Forest	65	0.139	0.130	0.79	39.6
2	<i>Amygdalus scoparia–Pistacia atlantica</i>	Forest	60	0.128	0.120	0.71	35.7
3	<i>Amygdalus scoparia–Pistacia khinj</i>	Forest	61	0.13	0.122	0.72	36.3
4	<i>Amygdalus scoparia–Daphne Spp</i>	Forest	62	0.132	0.124	0.73	36.9
5	<i>Cerasus Mahaleb – Cotoneaster Spp</i>	Forest	59	0.126	0.118	0.70	35.2
6	<i>Lonicera nummularia–Cerasus mahaleb</i>	Forest	60	0.128	0.112	0.71	35.7
7	<i>Pistacia atlantica–Cerasus mahaleb</i>	Forest	62	0.132	0.124	0.73	36.9
8	<i>Lonicera nummularia–Cerasus mahaleb</i>	Forest	61	0.13	0.122	0.72	36.3
9	<i>Pistacia atlantica–Cerasus mahaleb</i>	Forest	63	0.135	0.126	0.74	37.5
10	<i>Pistacia atlantica–Fraxinus rotund</i>	Forest	60	0.128	0.120	0.71	35.7
11	<i>Pistacia khinjuk</i>	Forest	58	0.124	0.116	0.78	39
12	<i>Quercus brantii</i>	Forest	57	0.122	0.114	0.76	38
13	<i>Quercus brantii–Acer monspessulanu</i>	Forest	61	0.13	0.122	0.72	36.3
14	<i>Quercus brantii–Amygdalus scoparia</i>	Forest	58	0.124	0.116	0.69	34.6
15	<i>Quercus brantii–Amygdalus Spp</i>	Forest	61	0.13	0.122	0.72	36.3
16	<i>Quercus brantii–Ficus Spp</i>	Forest	63	0.135	0.126	0.74	37.5
17	<i>Quercus brantii–Fraxinus rotundifo</i>	Forest	62	0.132	0.124	0.73	36.9
18	<i>Quercus brantii–Pistacia atlantica</i>	Forest	64	0.137	0.128	0.76	38.1
19	<i>Quercus brantii–Pistacia khinjuk</i>	Forest	62	0.132	0.124	0.73	36.9
20	<i>Ziziphus spina christi</i>	Forest	57	0.122	0.114	0.79	39.5
21	<i>Astragalus Spp.- Prennial grasses</i>	Range(Fair)	51	0.109	0.102	0.60	30.4
22	<i>Astragalus Spp.– Stipa Spp</i>	Range(Fair)	55	0.118	0.110	0.65	32.8
23	<i>Astragalus Spp.– Gundelia Spp</i>	Range(Fair)	53	0.113	0.106	0.63	31.6
24	<i>Astragalus Spp.– Daphnae Spp</i>	Range(Fair)	65	0.139	0.130	0.77	38.7
25	<i>Astragalus Spp.– Prangus Spp</i>	Range(Fair)	61	0.13	0.122	0.72	36.3

Table 2 The values of NPP, RUE, LUE, correlation between terrestrial data and CASA model (R^2) and percentage of NPP potential used in plant types of semi-humid climate

	Vegetation type	Life form (range condition)	NPP (gC/m ²)	LUE	RUE	R ²	NPP Change
1	<i>Amygdalus scoparia</i>	Forest	63	0.135	0.158	0.74	37.5
2	<i>Amygdalus scoparia—Pistacia khinjuk</i>	Forest	59	0.126	0.148	0.70	35.2
3	<i>Amygdalus scoparia—Acer monspessul</i>	Forest	58	0.124	0.145	0.69	34.6
4	<i>Amygdalus scoparia—Daphne Spp</i>	Forest	55	0.118	0.138	0.65	32.8
5	<i>Amygdalus scoparia—Ficus Spp</i>	Forest	54	0.115	0.135	0.64	32.2
6	<i>Cerasus mahaleb – Cotoneaster Spp</i>	Forest	55	0.118	0.138	0.65	32.8
7	<i>Lonicera nummularia—Cerasus mahale</i>	Forest	53	0.113	0.133	0.63	31.6
8	<i>Pistacia atlantica—Fraxinus rotund</i>	Forest	58	0.124	0.145	0.69	34.6
9	<i>Pistacia khinjuk</i>	Forest	60	0.128	0.150	0.71	35.7
10	<i>Quercus brantii</i>	Forest	61	0.13	0.153	0.72	36.3
11	<i>Quercus brantii—Crataegus Spp</i>	Forest	59	0.126	0.148	0.70	35.2
12	<i>Quercus brantii—Acer monspessulanu</i>	Forest	57	0.122	0.143	0.67	34
13	<i>Quercus brantii—Amygdalus scoparia</i>	Forest	54	0.115	0.135	0.64	32.2
14	<i>Quercus brantii—Amygdalus Spp</i>	Forest	55	0.118	0.138	0.65	32.8
15	<i>Quercus brantii—Ficus Spp</i>	Forest	53	0.113	0.133	0.63	31.6
16	<i>Quercus brantii—Fraxinus rotundifo</i>	Forest	57	0.122	0.143	0.67	34
17	<i>Quercus brantii—Pistacia atlantica</i>	Forest	56	0.12	0.140	0.66	33.4
18	<i>Quercus brantii—Pistacia khinjuk</i>	Forest	53	0.113	0.133	0.63	31.6
19	<i>Ziziphus spina christi</i>	Forest	52	0.111	0.130	0.73	36.5
20	<i>Annual grasses—Annual forbs</i>	Range(Poor)	30	0.064	0.075	0.53	26.5
21	<i>Astragalus Spp.– Daphnae Spp</i>	Range(Fair)	58	0.124	0.145	0.69	34.6
22	<i>Astragalus Spp.– Gundelia Spp</i>	Range(Fair)	48	0.103	0.120	0.57	28.6
23	<i>Astragalus Spp.– Prangus Spp</i>	Range(Fair)	51	0.109	0.128	0.60	30.4
24	<i>Astragalus—Prennial grasses</i>	Range(Fair)	36	0.077	0.090	0.42	21.5
25	<i>Astragalus Spp. – Stipa Spp</i>	Range(Fair)	56	0.12	0.140	0.66	33.4

lowest in semi-arid climates, *Quercus brantii* (0.40) was calculated as the highest and *Cornulaca Spp.- Annual grasses* (0.30) as the lowest in dry climates, *Populus Spp.–Tamarix Spp.* (0.35) was calculated as the highest and *Scirpus Spp.* (0.21) as the lowest, and in very arid climates, *Phragmetis Spp. – Tamarix Spp.* (0.33) was calculated as the highest and *Halocnemum Spp.–Aeluropus Spp.* (0.15) as the lowest.

NPP rate

The annual value of NPP in Khuzestan province was 0 to 114.6 (gC/m²), which showed a downward trend from east to west and north to south (Fig. 2). The NPP map showed that vegetation production started in March and peaked in May (0 to 47.9 (gC/m²), but from June vegetation production declined and stopped. According to the results (Fig. 3), The amount of NPP in *Amygdalus scoparia* (68 gC/m²) was the highest in very humid climates and then reached the lowest in hyper-arid regions as in *Halocnemum Spp.–Aeluropus Spp.* (15 gC/m²) the lowest NPP was observed. In general, the NPP decreased with decreasing humidity and rainfall. Therefore, the amount of

NPP in plant types was observed as follows: in very humid climates, the lowest and highest NPP levels were found in *Amygdalus scoparia* (68 gC/m²) and *Acantholimon Spp. – Astragalus Spp.* (59 gC/m²), respectively. In the humid region, the highest amount of NPP was found in *Amygdalus scoparia* (65 gC/m²) with tree vegetative form and the lowest in *Astragalus Spp.- Prennial grasses* (51 gC/m²) with plant vegetative form. In the semi-humid region, compared to the humid one, the amount of production was reduced so that the NPP reached 63 gC/m² in the *Amygdalus scoparia* to 63 gC/m² in the *Annual grasses – Annual forb.* With the decrease of humidity in Mediterranean climate, the amount of NPP in forested areas with tree cover decreased by about 9%, so that in *Quercus brantii*, the NPP value was about 54 gC/m², which by changing the vegetative form from tree to grass in *Annual grasses—Annual forbs* decreased to 25 gC/m². With decreasing humidity in the semi-arid region, the density of the tree vegetative form was observed relative to the rangeland and also the amount of NPP was observed from 49 gC/m² (*Quercus brantii*) to 18 gC/m² (*Annual grasses—Annual forbs*). In arid area, the vegetative form of the tree was only *Populus*

Table 3 The values of NPP, RUE, LUE, correlation between terrestrial data and CASA model (R^2) and percentage of NPP potential used in plant types of Mediterranean climate

	Vegetation type	Life form (range condition)	NPP (gC/m ²)	LUE	RUE	R ²	NPP Change
1	<i>Quercus brantii</i>	Forest	56	0.119	0.190	0.74	30
2	<i>Amygdalus scoparia</i>	Forest	55	0.118	0.184	0.74	30.6
3	<i>Amygdalus scoparia—Pistacia atlantica</i>	Forest	51	0.109	0.170	0.60	28.4
4	<i>Amygdalus scoparia—Pistacia khinj</i>	Forest	53	0.113	0.177	0.63	29.5
5	<i>Amygdalus scoparia—Acer monspessul</i>	Forest	52	0.111	0.174	0.61	28.9
6	<i>Amygdalus scoparia—Ficus Spp</i>	Forest	54	0.115	0.180	0.64	30
7	<i>Amygdalus Spp.—Quercus brantii</i>	Forest	53	0.113	0.177	0.63	29.5
8	<i>Cerasus mahaleb – Cotoneaster Spp</i>	Forest	51	0.109	0.177	0.60	28.4
9	<i>Quercus brantii—Acer monspessulanu</i>	Forest	51	0.109	0.170	0.60	28.4
10	<i>Quercus brantii—Amygdalus scoparia</i>	Forest	53	0.113	0.177	0.63	29.5
11	<i>Quercus brantii—Pistacia atlantica</i>	Forest	55	0.118	0.184	0.65	30.6
12	<i>Quercus brantii—Pistacia khinjuk</i>	Forest	52	0.111	0.174	0.61	28.9
13	<i>Ziziphus spina christi</i>	Forest	54	0.115	0.180	0.67	30
14	<i>Annual grasses—Annual forbs</i>	Range(Fair)	25	0.054	0.084	0.69	13.9
15	<i>Astragalus Spp.– Bromus Spp</i>	Range(Poor)	35	0.075	0.117	0.41	19.5
16	<i>Astragalus Spp.– Daphnae Spp</i>	Range(Fair)	48	0.103	0.160	0.57	26.7
17	<i>Astragalus Spp.– Gundelia Spp</i>	Range(Fair)	45	0.096	0.150	0.53	25
18	<i>Astragalus Spp.– Peganum Spp</i>	Range(Poor)	38	0.081	0.127	0.45	21.2
19	<i>Astragalus Spp. – Stipa Spp</i>	Range(Fair)	41	0.088	0.137	0.48	22.8
20	<i>Stipa Spp.– Helianthemum Spp</i>	Range(Poor)	32	0.069	0.107	0.38	17.8

Spp.—Tamarix Spp. with the NPP amount of 30 gC/m², which by changing the vegetative form and condition of the pasture was reduced to 12 gC/m² in *Annual grasses—Annual forbs*. In the hyper-arid regions, the vegetation production showed a downward trend so that the NPP value was found from 32 gC/m² (*Hammada Spp.*) to 11 gC/m² (*Suaeda Spp.—Seidlitzia Spp.*).

Investigation of light consumption and precipitation in plant types

Calculation of LUE and RUE indices showed that the efficiency of consumption in plant types is not the same in different climates, so that in a very humid area, the efficiency of light consumption and the effect of precipitation were higher than ultra-dry. In the very humid area, in *Amygdalus scoparia* the highest (0.145) and in *Suaeda Spp. – Seidlitzia Spp.* the lowest (0.035) LUE value was observed. The highest and lowest RUE values were found in *Amygdalus scoparia* and *Suaeda Spp.—Seidlitzia Spp.* The LUE index decreased with decreasing rainfall in different climates, so that the LUE value range was from 0.145 in *Amygdalus scoparia* to 0.059 in *Astragalus Spp.—Gundelia Spp.* in very humid area, from 0.139 in *Amygdalus scoparia* to 0.102 in *Astragalus Spp.—Perennial grasses* in humid area, from 0.135 in *Amygdalus scoparia* to 0.064 in *Annual grasses—Annual forbs*

in semi-humid area, from 0.119 in *Quercus brantii* to 0.054 in *Annual grasses—Annual forbs* in Mediterranean area, from 0.108 in *Quercus brantii* to 0.039 in *Annual grasses—Annual forbs* in semi-dry area, from 0.064 in *Populus Spp.—Tamarix Spp.* to 0.026 in *Annual grasses—Annual forbs* in dry area and from 0.068 in *Hammada Spp.* to 0.038 in *Suaeda Spp.—Seidlitzia Spp.* in ultra-dry area.

RUE values varied depending on the type of vegetation, the climate of the region as well as the topographic conditions. So that more RUE values were observed in very humid areas than dry and ultra-dry ones. In very humid climates, the RUE index was higher in forest areas than in rangelands. The RUE value range was from 0.114 in *Amygdalus scoparia* to 0.075 in *Astragalus Spp.—Gundelia Spp.* in very humid area, from 0.139 in *Amygdalus scoparia* to 0.102 in *Astragalus Spp.—Perennial grasses* in humid area, from 0.158 in *Amygdalus scoparia* to 0.075 in *Annual grasses—Annual forbs* in semi-humid area, from 0.19 in *Quercus brantii* to 0.085 in *Annual grasses—Annual forbs* in Mediterranean area, from 0.196 in *Quercus brantii* to 0.075 in *Annual grasses—Annual forbs* in semi-dry area, from 0.177 in *Populus Spp.—Tamarix Spp.* to 0.071 in *Annual grasses—Annual forbs* in dry area and from 0.246 in *Hammada sp.* to 0.138 in *Suaeda Spp.—Seidlitzia Spp.* in ultra-dry area.

Table 4 The values of NPP, RUE, LUE, correlation between terrestrial data and CASA model (R^2) and percentage of NPP potential used in plant types of semi-dry, dry, and ultra-dry climate

	Climate Type	Vegetation type	Life form (range condition)	NPP (gC/m ²)	LUE	RUE	R ²	NPP Change
1	semi-dry	<i>Amygdalus scoparia—Ficus Spp</i>	Forest	46	0.098	0.184	0.54	38.4
2	semi-dry	<i>Amygdalus Spp.—Quercus brantii</i>	Forest	45	0.096	0.180	0.53	37.5
3	semi-dry	<i>Amygdalus Spp</i>	Forest	47	0.100	0.188	0.68	39.2
4	semi-dry	<i>Quercus brantii</i>	Forest	49	0.105	0.196	0.65	40.9
5	semi-dry	<i>Quercus brantii—Acer monspessulanu</i>	Forest	47	0.100	0.188	0.55	39.2
6	semi-dry	<i>Quercus brantii—Amygdalus scoparia</i>	Forest	43	0.092	0.172	0.51	35.9
7	semi-dry	<i>Quercus brantii—Pistacia atlantica</i>	Forest	44	0.094	0.176	0.52	36.7
8	semi-dry	<i>Ziziphus spina christi</i>	Forest	40	0.086	0.160	0.47	33.4
9	semi-dry	<i>Annual grasses—Annual forbs</i>	Range(Fair)	18	0.039	0.072	0.50	15
10	semi-dry	<i>Astragalus – Bromus Spp</i>	Range(Poor)	28	0.06	0.112	0.33	23.4
11	semi-dry	<i>Astragalus Spp. – Centaurea Spp</i>	Range(Poor)	36	0.077	0.144	0.42	30
12	semi-dry	<i>Astragalus Spp.– Daphnae Spp</i>	Range(Fair)	44	0.094	0.176	0.52	36.7
13	semi-dry	<i>Astragalus Spp. – Euphorbia Spp</i>	Range(Fair)	41	0.088	0.164	0.48	34.2
14	semi-dry	<i>Astragalus Spp.– Gundelia Spp</i>	Range(Fair)	43	0.092	0.172	0.51	35.9
15	semi-dry	<i>Astragalus Spp.– Peganum Spp</i>	Range(Fair)	38	0.081	0.152	0.45	31.7
16	semi-dry	<i>Astragalus Spp. – Stipa Spp</i>	Range(Fair)	37	0.079	0.148	0.44	30.9
17	semi-dry	<i>Cornulaca Spp.- Annual grasses</i>	Range(Poor)	26	0.056	0.104	0.30	21.7
18	semi-dry	<i>Gymnocarpus Spp.– Astragalus Spp</i>	Range(Poor)	32	0.069	0.128	0.38	26.7
19	semi-dry	<i>Stipa Spp.– Helianthemum Spp</i>	Range(Fair)	29	0.062	0.116	0.55	24.2
20	dry	<i>Populus Spp.– Tamarix Spp</i>	Forest	30	0.064	0.177	0.35	30
21	dry	<i>Annual grasses—Annual forbs</i>	Range(Poor)	12	0.026	0.071	0.30	12
22	dry	<i>Artemisia sieberi – Cornulaca Spp</i>	Range(Poor)	22	0.047	0.130	0.26	22
23	dry	<i>Artemisia sieberi – Gymnocarpus Spp</i>	Range(Poor)	26	0.056	0.153	0.31	26
24	dry	<i>Artemisia sieberi – Scariola Spp</i>	Range(Poor)	23	0.049	0.136	0.27	23
25	dry	<i>Astragalus Spp.– Euphorbia Spp</i>	Range(Fair)	25	0.054	0.148	0.30	25
26	dry	<i>Astragalus Spp.- Preennial grasses</i>	Range(Fair)	23	0.049	0.136	0.27	23
27	dry	<i>Astragalus Spp. – Stipa Spp</i>	Range(Poor)	20	0.043	0.118	0.24	20
28	dry	<i>Atriplex Spp. – Salsola Spp</i>	Range(Poor)	28	0.06	0.165	0.33	28
29	dry	<i>Cornulaca Spp.- Annual grasses</i>	Range(Poor)	26	0.056	0.153	0.31	26
30	dry	<i>Cornulaca Spp.– Artemisia Spp</i>	Range(Poor)	24	0.052	0.142	0.28	24
31	dry	<i>Gymnocarpus Spp.– Astragalus Spp</i>	Range(Poor)	22	0.047	0.130	0.26	22
32	dry	<i>Halocnemum Spp. – Aeluropus Spp</i>	Range(Poor)	27	0.058	0.159	0.32	27
33	dry	<i>Halocnemum Spp.– Salsola Spp</i>	Range (Very poor)	20	0.043	0.118	0.24	20
34	dry	<i>Hammada Spp</i>	Range(Poor)	29	0.062	0.171	0.34	29
35	dry	<i>Phragmetis Spp. – Tamarix Spp</i>	Range(Poor)	16	0.035	0.095	0.30	16
36	dry	<i>Platychaete Spp. – Cymbopogon Spp</i>	Range(Poor)	24	0.052	0.142	0.28	24
37	dry	<i>Salsola Spp.– Helianthemum Spp</i>	Range(Poor)	19	0.041	0.112	0.22	19
38	dry	<i>Salsola Spp</i>	Range(Poor)	20	0.043	0.118	0.24	20
39	dry	<i>Scirpus Spp</i>	Range(Poor)	18	0.039	0.106	0.21	18
40	dry	<i>Seidlitzia Spp</i>	Range(Poor)	20	0.043	0.118	0.38	20
41	dry	<i>Stipa Spp.– Bromus Spp</i>	Range(Poor)	15	0.032	0.089	0.35	15
42	dry	<i>Stipa Spp.– Helianthemum Spp</i>	Range(Poor)	19	0.041	0.112	0.22	19
43	dry	<i>Suaeda Spp.– Seidlitzia Spp</i>	Range(Poor)	27	0.058	0.159	0.32	27
44	ultra-dry	<i>Halocnemum Spp. – Aeluropus Spp</i>	Range (Very poor)	23	0.053	0.192	0.15	31.3
45	ultra-dry	<i>Halocnemum Spp.– Salsola Spp</i>	Range(Poor)	30	0.063	0.230	0.30	37.5
46	ultra-dry	<i>Hammada Spp</i>	Range(Poor)	32	0.068	0.246	0.31	40
47	ultra-dry	<i>Phragmetis Spp.– Tamarix Spp</i>	Range(Fair)	28	0.059	0.215	0.33	35
48	ultra-dry	<i>Scirpus Spp</i>	Range(Poor)	20	0.042	0.153	0.29	25

Table 4 (continued)

	Climate Type	Vegetation type	Life form (range condition)	NPP (gC/m ²)	LUE	RUE	R ²	NPP Change
49	ultra-dry	<i>Seidlitzia Spp</i>	Range(Poor)	21	0.044	0.161	0.28	26.3
50	ultra-dry	<i>Suaeda Spp.– Seidlitzia Spp</i>	Range(Poor)	11	0.038	0.138	0.26	22.5

Potential of NPP

The produced map showed that the potential of NPP in this region is between 51 and 250 gC/m². Therefore, the difference between NPP and climatic potential varied depending on climatic conditions and topography. According to the obtained results (Fig. 4), the difference between the values in very humid climates was 27.2% (*Amygdalus scoparia*) to 14% (*Astragalus Spp.–Gundelia Spp.*) in very humid climate conditions, 39.6% (*Amygdalus scoparia*) up to 30% (*Astragalus Spp.–Gundelia Spp.*) in humid climate conditions, 37.5% (*Amygdalus scoparia*) to 26% (*Annual grasses—Annual forbs*) in semi-humid climate conditions,

30% (*Quercus brantii*) to 13.9% (*Annual grasses—Annual forbs*) in Mediterranean climate conditions, 38% (*Quercus brantii*) to 15% (*Annual grasses—Annual forbs*) in semi-arid climate conditions, 30% (*Populus Spp.- Tamarix Spp.*) to 12% (*Annual grasses—Annual forbs*) in dry climate conditions and 40% (*Hammada sp.*) up to 25% (*Scirpus Spp.*) in ultra-dry climate conditions. Many changes were observed in plant types depending on the type of vegetative form.

Discussion

Although NPP at the level of arid climates in Central Iran can not be assessed with MODIS sensor data such as MOD17A3H, the results of the present study showed that this feature can be modeled with the help of MODIS images. However, the degree of correlation between terrestrial and simulated data was different based on climatic conditions and plant type (Tables 1, 2, 3 and 4). In humid areas, there was the highest correlation between terrestrial and simulated data, which can be attributed to the existence of suitable conditions in terms of soil moisture and soil humus (Churkina et al. 1999; Froelking et al. 1998) (Table 1). In these areas, the rate of leaf area index and photosynthesis, and consequently the amount of NPP, increases. With soil dryness, the amount of leaf area index, photosynthetic reflection of plants and its relationship with plant indices (NDVI) and simulated models such as CASA also decrease while it has been proven in various observations (Coughenour 1999; Hunt Jr et al. 2003). In addition, the comparison of plant types in a similar climate showed that the production of plant types with medium rangeland condition has a higher correlation with CASA model than poor rangeland condition which has been stated by Hadian et al. (2019) due to reduced fertility, leaf area and greenness. Temperature, precipitation and solar energy factors play major role in plant production (Yaghmaei et al. 2020). Zarei et al (2021) also presented that temperature, precipitation and evapotranspiration effect on the estimation of NPP. At the beginning of the season, there is a temperature limit on plant growth, so compared to the middle of the growing season, the vegetation production rate was lower (Table 1). As the weather warms, the amount of NPP also increases, so that in June it rises from 0–47 gC/m² to 0–11 gC/m². By reducing the amount of soil moisture, vegetation production

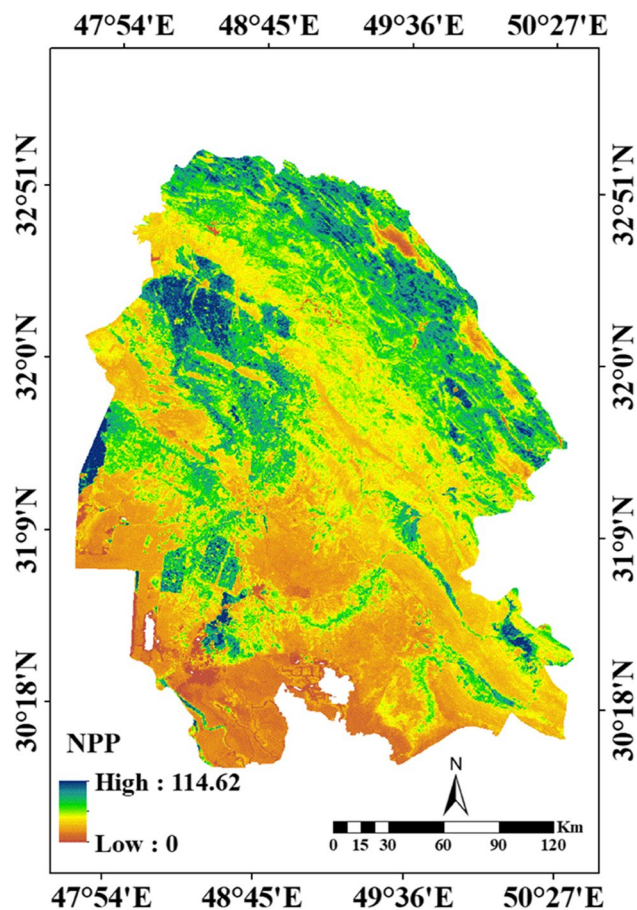


Fig. 2 Spatial distribution of NPP in Khuzestan province in 2000–2021

Fig. 3 The monthly spatial and temporal variation of NPP in 2000–2021

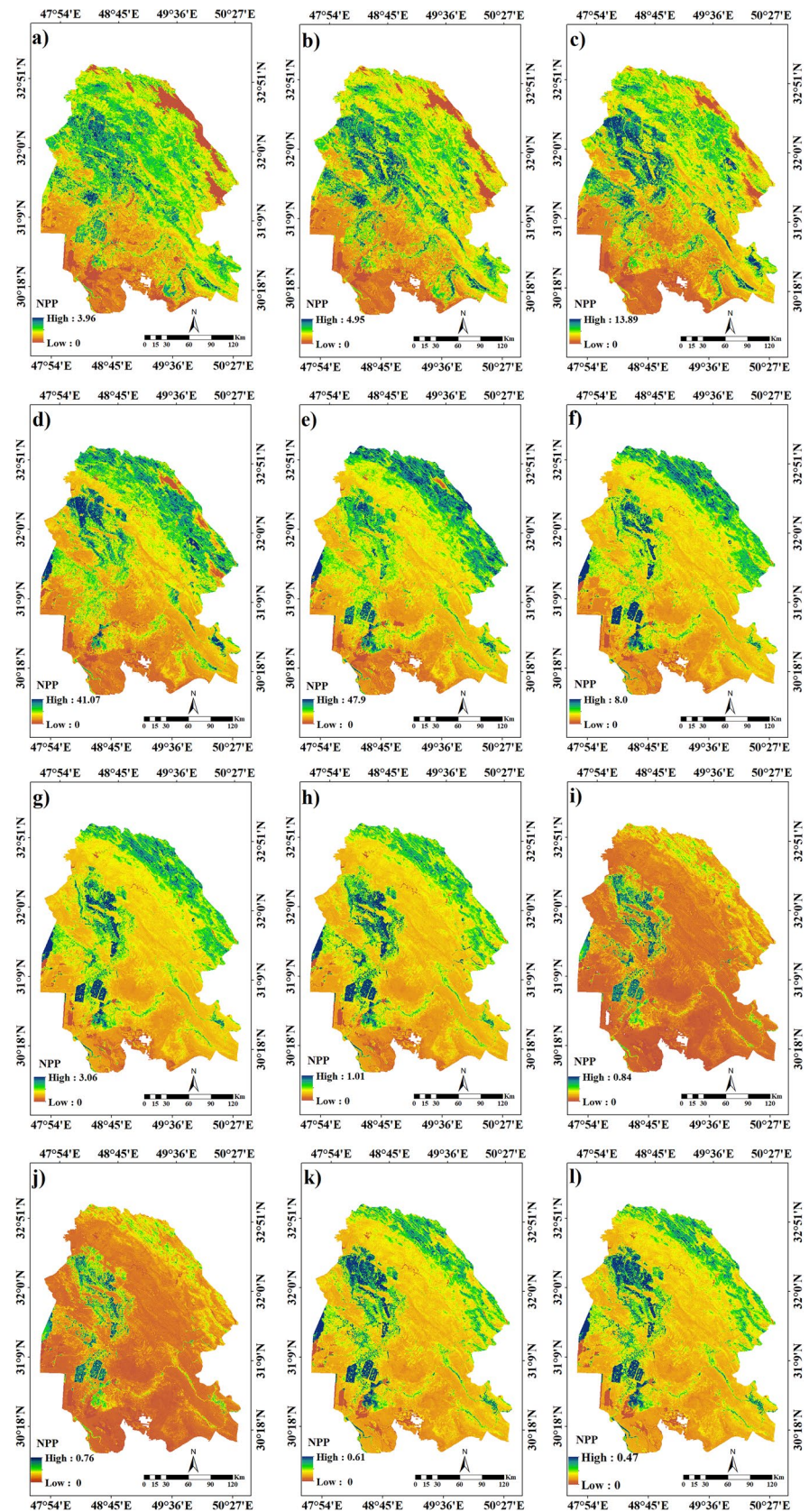
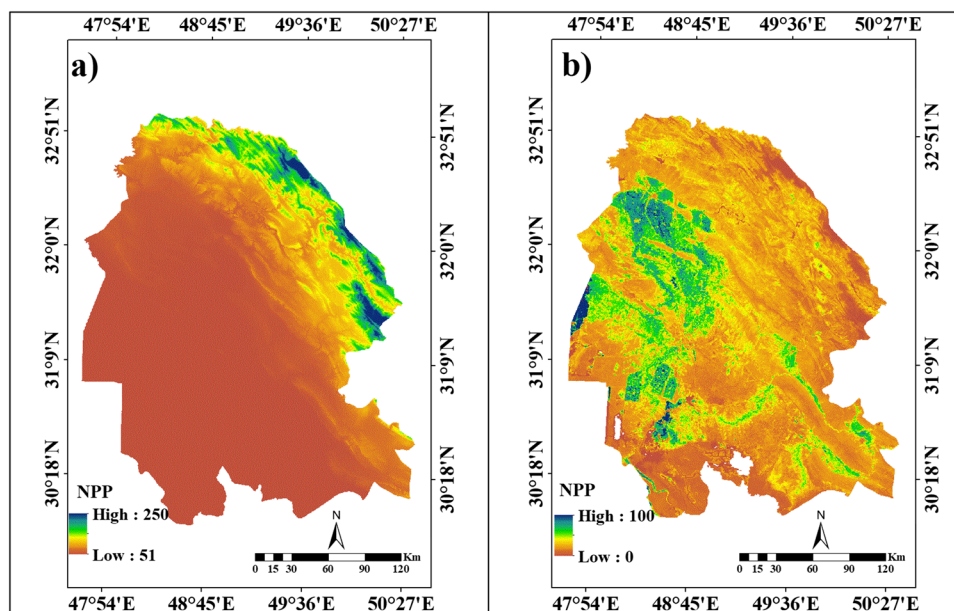


Fig. 4 a) The map of climatic potential of NPP map and b) the percentage of NPP to climatic potential



almost stops. Therefore, the two factors of temperature and precipitation can be expressed as determining elements of NPP in the early and late growing season, respectively, which has also been confirmed by Xing et al. 2021. Xiao et al. (2022) also presented that the increased precipitation and temperature would enhance the vegetation growth. It seems that in arid and semi-arid regions, soil moisture from the middle of the growing season is the most important factor in NPP, which is also affected by the type of soil in the region (Jha and Srivastava 2018). In degraded areas, soil erosion reduces the amount of soil pores and the amount of moisture in it decreases (Ibrahim et al. 2015). Therefore, in rangelands with poor and very poor rangeland condition, with eroded soil, the length of plant growth and production period decreases (Francis et al. 1986).

According to the results (Table 2) *Amygdalus scoparia* with tree vegetative form, had the highest NPP value (68 gC/m²) because due to specific climatic conditions, the depth of the fertile layer in humid and semi-humid areas was higher compared to arid and semi-arid areas and this creates the conditions for the growth of tree plants with deeper roots. Therefore, in humid areas, there is a greater ability to produce vegetation rather than arid and semi-arid areas. This matter has been demonstrated by Thorne and Frank (2009). Moreover, having deep roots in trees allows them to use deeper water and increase their resistance to drought changes (Yanagisawa and Fujita 1999). However, the possibility of using the moisture of the lower layers of the soil is reduced in shrubs due to their root structure, as the amount of NPP per plant decreases, which has been confirmed by Kizito et al. 2006. In addition, plant types in different climates from humid to dry, do not have the same conditions in terms of production per unit area, and

different densities of vegetation were observed based on the amount of moisture. *Astragalus Spp.* were different in terms of production per unit area in humid and ultra-dry areas. Geographical location and climatic diversity in the study area has led to the emergence of different plant types (Han et al. 2023a, b). The plant species of *Amygdalus scoparia* and *Suaeda Spp.*–*Seidlitzia Spp.* were observed from east to west with the NPP values of 68 gC/m² and 11 gC/m², respectively. Comparison of topographic and NPP maps showed that topographic changes play an important role in vegetation production, which can be attributed to rainfall fluctuations due to topography and soil moisture, so that in various observations, rainfall changes due to topography have been mentioned (Navale and Singh 2020). As the amount of precipitation increases, the NPP values also increase, so it is possible to express the changes in NPP values in the region due to rainfall fluctuations as the result of physiographic conditions of the region (Han et al. 2023a, b). Limiting temperature and precipitation in the early and late growing season reduces LUE (Wang et al. 2022), so in each plant type, depending on the climate and type of plant, different amounts of LUE were observed (Wen et al. 2019). In degraded plant types, the amount of LUE was also reduced compared to rangelands with good and average condition. Of course, this factor also varies depending on the type of vegetative form. According to the present observations (Table 3), plant types with tree vegetative form had higher LUE values than rangelands, which is also due to their deep roots and reduced soil moisture at the end of the season. In rangelands, shrub types had higher LUE values than annuals and grasses (Del Grosso et al. 2008).

According to other studies (Yang et al. 2003; Suseela et al. 2012), in each climate condition, depending on temperature and humidity conditions, there is a certain amount of production potential, but soil conditions and rangeland degradation cause that lower percentage of production potential be used. The results of the present study showed that in humid areas with mountainous topography and high slope, a large part of the rainfall received as runoff is lost, which increases with the destruction of vegetation and a decrease in the percentage of vegetation. Therefore, in humid and mountainous areas (Table 4) less percentage of climatic potential is used. However, in arid and hyper-arid regions, due to the adaptation of plants, such as increasing root length to phytomass, the efficiency of using the moisture in the soil depth and as a result, the production potential increases. Therefore, in different climates, the percentage of use of climatic potential (Table 4) was different, which was also confirmed by Bonfante, Terribile, and Bouma (2019). In this region, the values of RUE index were also different. So that in the degraded types compared to the average plant types, the rainfall efficiency decreased (Table 4) which can be attributed to factors such as erosion and destruction of soil structure (Wessels et al. 2007). However, in arid and hyper-arid regions, biological strategy causes plants to make maximum use of soil moisture with the development of root structure, while minimizing the amount of evapotranspiration by morphological changes (Li et al. 2015). In this area, the degradation is high and data with an accuracy of 250 m² has been used. Landsat images with an accuracy of 30 m² can be used in future studies to increase the accuracy. On the other hand, the possibility of errors in rainfall data as well as the limited number of stations in some areas increases the uncertainties.

This research has been done with the help of MODIS satellite images to separate plant types in climatic classes, which include factors of rangeland status, vegetation conditions and soil. Also, in this study, by calculating the climatic potential of plant production, the degradation status of vegetation has been shown, which has rarely been considered in previous studies. This study was conducted in a coastal area, which also shows the effects of topography in determining the existing climatic classes and vegetation, which has not been done before in similar areas.

Conclusion

The present study was conducted to investigate and model the NPP in plant types in the rangelands of Khuzestan province with the help of MODIS images and to evaluate the efficiency of plant photosynthesis in different climates of this region. This study was conducted specifically to map NPP of Khuzestan province with the CASA model

over a 21-year period from 2000–2021 along with its accuracy evaluation adopting field data on the scale of the climate zones. However, the degree of correlation between terrestrial and simulated data was different based on climatic conditions and plant type.

The changes in climatic regions play an important role in vegetation production of the area. Therefore, the climate condition from very humid and cold to ultra-dry in Khuzestan province has led to the emergence of various plant species with different vegetative forms that have good to very poor rangeland status. The comparison of plant types in a similar climate showed that the production of plant types with medium rangeland condition has a higher correlation with CASA model than poor rangeland condition. Temperature, precipitation and evapotranspiration effect on the estimation of NPP, while the increased precipitation and temperature would enhance the vegetation growth. In addition, plant types in different climates from humid to dry, do not have the same conditions in terms of production per unit area.

This study presented that modeling and up-to-date satellite images have a high capability in estimating and investigating the spatial and temporal distribution of production in vegetative climates. Early knowledge of the process of changes in actual production and potential can inform managers of the rangeland situation and its negative or positive trend and changes in the status of important rangeland species and make better decisions for the region's future.

Acknowledgements This study was funded by Iran National Science Foundation (INSF). We are grateful to the INSF for financial supporting of the research with the grant No. 99011835.

Authors' contributions A.A. was the supervisor. A.A. and F. H. were the designer of the hypotheses, wrote the text of the article and interpreted the data. S.S. and L.Y. helped to interpret part of data and all authors substantively revised the text. A.A. and S.S. edited the English language.

Declarations

Competing interests The authors of the manuscript titled "Investigating Net Primary Production in Climate Regions of Khuzestan Province, Iran using CASA model" declare that they have no competing interests.

References

- Bajgiran PR, Darvishsefat AA, Khalili A, Makhdom MF (2008) Using AVHRR-based vegetation indices for drought monitoring in the Northwest of Iran. *J Arid Environ* 72(6):1086–1096
- Bradford J, Hicke J, Lauenroth W (2005) The relative importance of light-use efficiency modifications from environmental conditions and cultivation for estimation of large-scale net primary productivity. *Remote Sens Environ* 96(2):246–255

- Chen J, Liu J, Cihlar J, Goulden M (1999) Daily canopy photosynthesis model through temporal and spatial scaling for remote sensing applications. *Ecol Model* 124(2–3):99–119
- Chen Z, Chen J, Xu G, Sha Z, Yin J, Li Z (2023) Estimation and Climate Impact Analysis of Terrestrial Vegetation Net Primary Productivity in China from 2001 to 2020. *Land* 12(6):1223
- Costanza R (2012) Ecosystem health and ecological engineering. *Ecol Eng* 45:24–29
- Cramer W, Bondeau A, Woodward FI, Prentice IC, Betts RA, Brovkin V, Cox PM, Fisher V, Foley JA, Friend AD (2001) Global response of terrestrial ecosystem structure and function to CO₂ and climate change: results from six dynamic global vegetation models. *Glob Change Biol* 7(4):357–373
- Darvish Sefat A, Zare A (1998) Assessment of Availability of satellite data for mapping of vegetation in arid and semi-arid regions. *J Nat Resour Iran* 50(20):47–52 (In Farsi)
- Diegues H, Paruelo JM (2017) Disentangling the signal of climatic fluctuations from land use: changes in ecosystem functioning in South American protected areas (1982–2012). *Remote Sens Ecol Conserv* 3(4):177–189
- Diouf A, Lambin E (2001) Monitoring land-cover changes in semi-arid regions: remote sensing data and field observations in the Ferlo, Senegal. *J Arid Environ* 48(2):129–148
- Field CB, Randerson JT, Malmström CM (1995) Global net primary production: combining ecology and remote sensing. *Remote Sens Environ* 51(1):74–88
- Fischer D, Chapman S, Classen AT, Gehring C, Grady K, Schweitzer J, Whitham T (2014) Plant genetic effects on soils under climate change. *Plant Soil* 379(1–2):1–19
- Fu S, Zhou Y, Lei J, Zhou N (2023) Changes in the spatiotemporal of net primary productivity in the conventional lake chad basin between 2001 and 2020 based on CASA model. *Atmosphere* 14(2):232
- Gao F, Hilker T, Zhu X, Anderson M, Masek J, Wang P, Yang Y (2015) Fusing Landsat and MODIS data for vegetation monitoring. *IEEE Geosci Remote Sens Mag* 3(3):47–60
- Hadian F, Jafari R, Bashari H, Tartesh M, Clarke KD (2019) Estimation of spatial and temporal changes in net primary production based on Carnegie Ames Stanford Approach (CASA) model in semi-arid rangelands of Semirom County, Iran. *J Arid Land* 11(4):477–494
- Han F, Yu C, Fu G (2023) Asymmetric warming among elevations may homogenize plant α -diversity and aboveground net primary production of alpine grasslands. *Front Ecol Evol* 11:1126651
- Han F, Yu C, Fu G (2023) Non-growing/growing season non-uniform-warming increases precipitation use efficiency but reduces its temporal stability in an alpine meadow. *Front Plant Sci* 14:1090204
- He Y, Piao S, Li X, Chen A, Qin D (2018) Global patterns of vegetation carbon use efficiency and their climate drivers deduced from MODIS satellite data and process-based models. *Agric for Meteorol* 256:150–158
- He T, Dai Z, Li W, Zhou J, Zhang J, Li C, Dai T, Li W, Lu H, Ye Y, Xu L, Jiang Z (2023) Response of net primary productivity of vegetation to drought: A case study of Qinba Mountainous area, China (2001–2018). *Ecol Ind* 149:110148
- Imhoff ML, Bounoua L, Ricketts T, Loucks C, Harriss R, Lawrence WT (2004) Global patterns in human consumption of net primary production. *Nature* 429(6994):870
- Ke J, Zhou D, Hai C, Yu Y, Jun H, Li B (2022) Temporal and spatial variation of vegetation in net primary productivity of the Shendong coal mining area, Inner Mongolia Autonomous Region. *Sustainability* 14(17):10883
- Khajeddin SJ (1995) A survey of the plant communities of the Jazmorian, Iran, using Landsat MSS data. University of Reading, Pages
- Liu S, Bliss N, Sundquist E, Huntington TG (2003) Modeling carbon dynamics in vegetation and soil under the impact of soil erosion and deposition. *Glob Biogeochem Cycles* 17(2):1–24
- Peng J, Shen H, Wu W, Liu Y, Wang Y (2016) Net primary productivity (NPP) dynamics and associated urbanization driving forces in metropolitan areas: A case study in Beijing City, China. *Landsc Ecol* 31(5):1077–1092
- Ruimy A, Saugier B, Dedieu G (1994) Methodology for the estimation of terrestrial net primary production from remotely sensed data. *J Geophys Res Atmos* 99(D3):5263–5283
- Ruimy A, Kergoat L, Bondeau A, Intercomparison TPOTPNM (1999) Comparing global models of terrestrial net primary productivity (NPP): Analysis of differences in light absorption and light-use efficiency. *Glob Change Biol* 5(S1):56–64
- United Nations Statistics Division (2020) Sustainable Development Goals (SDGs) Report. <https://unstats.un.org/sdgs/report/2020/>
- Wang J, Li M, Fu G (2022) The change in environmental variables linked to climate change has a stronger effect on aboveground net primary productivity than does phenological change in alpine grasslands. *Front Plant Sci* 12:798633
- Xiao F, Liu Q, Xu Y (2022) Estimation of terrestrial net primary productivity in the Yellow river basin of China using light use efficiency model. *Sustainability* 14:7399
- Yaghmaei L, Soltani S, Jafari R (2020) Spatiotemporal Response of Rangeland NPP to Drought in Central Iran based on SPDI Index. *Contemp Probl Ecol* 13(6):694–707
- Yaghmaei L, Jafari R, Soltani S (2021) Investigating net primary production in climate regions of central Zagros, Iran, using MODIS and meteorological data. *Clim Res* 83:173–186
- Yu D, Shi P, Shao H, Zhu W, Pan Y (2009) Modelling net primary productivity of terrestrial ecosystems in East Asia based on an improved CASA ecosystem model. *Int J Remote Sens* 30(18):4851–4866
- Yuan J, Niu Z, Wang C (2006) Vegetation NPP distribution based on MODIS data and CASA model—A case study of northern Hebei Province. *Chin Geogra Sci* 16(4):334–341
- Zarei A, Chemura A, Gleixner S, Hoff H (2021) Evaluating the grassland NPP dynamics in response to climate change in Tanzania. *Ecol Ind* 125:107600
- Zha X, Niu B, Li M, Duan C (2022) Increasing impact of precipitation on alpine-grassland productivity over Last two decades on the Tibetan Plateau. *Remote Sens* 14(14):3430
- Zhang L, Lü Y, Fu B, Dong Z, Zeng Y, Wu B (2017) Mapping ecosystem services for China's ecoregions with a biophysical surrogate approach. *Landsc Urban Plan* 161:22–31

Springer Nature or its licensor (e.g. a society or other partner) holds exclusive rights to this article under a publishing agreement with the author(s) or other rightsholder(s); author self-archiving of the accepted manuscript version of this article is solely governed by the terms of such publishing agreement and applicable law.